

**IMPROVEMENTS IN MONITORING OF SMALL REGIONAL EVENTS  
BASED ON GROUND TRUTH DATA IN TURKEY AND ISRAEL**

Vladimir Pinsky,<sup>1</sup> Yefim Gitterman,<sup>1</sup> Avi Shapira,<sup>1</sup> Mehmet Ergin,<sup>2</sup> and Cemil Gurbuz<sup>3</sup>

Geophysical Institute of Israel (GII);<sup>1</sup> TUBITAK Marmara Research Center;<sup>2</sup>  
Bogazici University, Kandilli Observatory and Earthquake Research Institute (KOERI)<sup>3</sup>

Sponsored by Defense Threat Reduction Agency

Contract No. DTRA01-00-C-0119

**ABSTRACT**

To upgrade local crust models and estimate site-specific station corrections (SSSCs) for more accurate hypocenter location, a number of controlled quarry blasts (GT0) were recently conducted in the Marmara Sea region, close to the Izmit earthquake (17 August 1999). Both the blasts and well-constrained aftershocks (GT5) were recorded by the KOERI network and TUBITAK stations in Turkey. The blasts were located using arrival times and two 1-D crustal models: 1) the KOERI model for regional location; 2) a modified model from refraction profiles. Improvement was achieved by using model 2 and VELEST, an optimization procedure. The improved models were used to relocate selected Izmit aftershocks. Relocation experiments, including calculation of the hypocenter ellipsoid and Monte-Carlo simulation, were performed to verify accuracy and reliability of new hypocenter estimations.

We continued the program of calibration explosions in Israel, conducting a series of controlled quarry blasts to the North of the Sea of Galilee, including a 25-ton shot to complement the 2002 Rotem explosion in the Negev desert, providing better signal observations in Cyprus, Lebanon, Syria and Turkey. The closely spaced (~50 km) 1999 Dead Sea and 25-ton Rotem calibration explosions were recorded at the same stations in Israel, Jordan, Cyprus and Saudi Arabia, providing observations for similar propagation paths. The data enabled an analysis of the influence of different sources on amplitudes, waveform and spectral content of regional phases. The calibration explosions, located in the Dead Sea fault zone, provided a variety of results in the context of nuclear test monitoring: a) accurate travel time corrections for regional phases relative to IASPEI91 and GII models at stations of local networks and the International Monitoring System (IMS), b) verification and improvement of velocity models, c) estimation of attenuation and magnitude-yield relations, d) characterization of new seismic sources and local mining practices, and multi-station discrimination analysis.

We provided a pilot performance analysis for a new IMS array on Mt. Meron, Israel (MMAI or AS49), operational in January 2003. The 16-element small aperture array is equipped with broadband Gurlap seismometers placed in deep (50 –100 m) boreholes. The MMAI detectability and signal parameter estimation was analyzed by the standard and adaptive beamforming techniques using data from the recent controlled quarry explosion series in Israel and regional GT5 earthquakes. New robust beamforming techniques have been developed and applied to the array data, showing promising results for enhancing monitoring capabilities in the region.

The 2Dtracern software was used to compute SSSCs of the Pg, Pn, P, Sg, Sn, S phases for the eight stations: EIL, MRNI, BRAR, DAVOS, KVAR, MLR, GERESS and OBN, using the 3D velocity model CUB1.0. For stations EIL, MRNI and BRAR we have computed SSSCs in the direction of small areas in Cyprus and Turkey (Izmit, Duzce and Adana), containing selected Ground Truth (GT0-GT5) sources. The results have been compared to the observed deviations between the measured and IASPEI91 travel times from the ground-truth (GT) events.

**OBJECTIVE**

The main objective is to characterize and enhance the nuclear explosion monitoring potential in the eastern Mediterranean area through building a regional knowledge base, including upgrading local crust models, and estimating site-specific station corrections for more accurate hypocenter locations, using ground-truth events.

**RESEARCH ACCOMPLISHED**

**Marmara Controlled GT0 Blasts and Location Analysis**

To upgrade local crust models and estimate site-specific station corrections for more accurate hypocenter locations, a number of controlled quarry blasts (GT0) were recently conducted in the Marmara Sea region.

Numerous seismic events in the Istanbul area (east and southeast of the Marmara Sea) were recorded at KOERI and TUBITAK stations during the past two years (Figure 1a). The data analysis shows that not all of them are earthquakes, because the distribution of events does not follow the known fault systems. A survey of the area revealed quarries conducting regular production blasts (Figure 1b). Most of these quarries are located to the east of Istanbul.

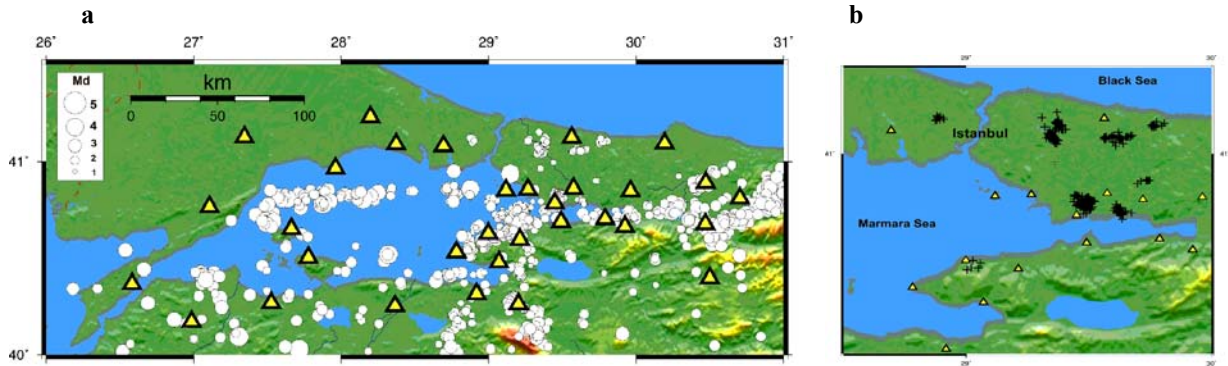


Figure 1. Epicenter distribution in the Marmara Region (2001-2002) (a), and explosion clusters near Istanbul (b).

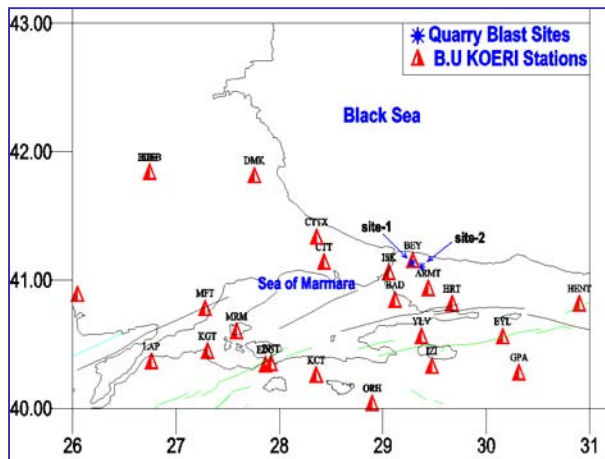


Figure 2. Map of quarry blast sites and local recording stations.

The KOERI project team visited some of the areas and found that large explosions were conducted in two locations (Figure 2). We measured the coordinates, recorded origin times and collected blast design parameters (see Table 1). First arrival times were measured with seismic sensors (equipped with GPS) placed near (50–100 m) the blast site, providing relatively accurate estimates of origin (detonation) time.

Because the blasts are single-fired there is no delay between holes. Several blasts with ground-truth (GT0) information were recorded at distances up to 80 km from the shot point by the KOERI seismic network stations (Figure 3). We used this data to perform the location analysis.

The quarry site location was estimated based on the arrival times and three crustal models for the study area (Table 2): 1) the KOERI starting model 1 which is used in the Kandilli laboratory to locate earthquakes in and around Turkey; 2) the

KOERI modified model obtained from ray-tracing modeling of refraction studies in the region; and 3) the TUBITAK crustal model.

**Table 1. Parameters of the controlled Marmara quarry blasts.**

#	Quarry site	Date	Origin time	Closest station, km	Charge, kg	Hole depth,m	Number of holes
1	#1-Soyak	31.07.2002	12:50:01.79	~4(BEY)	1030	7	14
2	41.102N 29.375E	05.08.2002	13:38:41.80	0.1	1300	8	16
3	#2-Lafarge	14.08.2002	10:15:40.55	~4(BEY)	735	8	41
4	41.116N	14.08.2002	10:24:17.70	~4(BEY)	800?	-	-
5	29.295E	16.08.2002	09:15:11.55	0.05	210	8	15
6		26.08.2002	09:28:33.20	~4(BEY)	900?	-	-

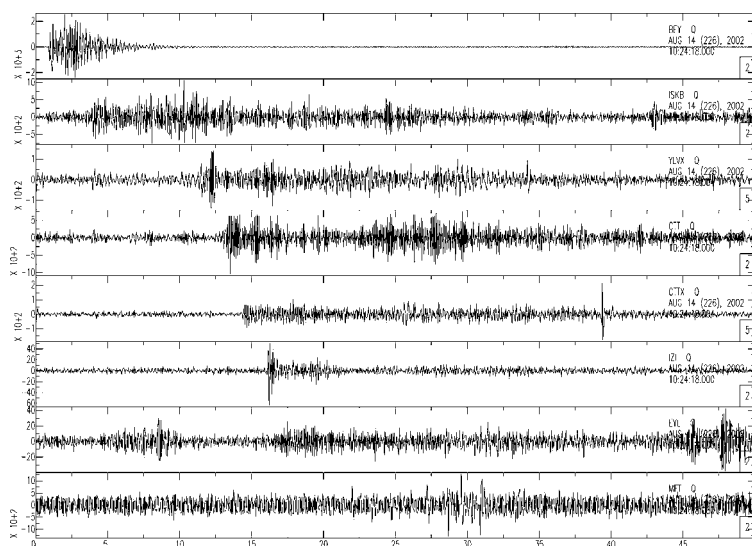


**Figure 3. Seismograms of the Marmara blast No.4 (14.08.2002) recorded at KOERI stations used for the location analysis.**

**Table 2. Crustal models used for the Marmara blasts location analysis.**

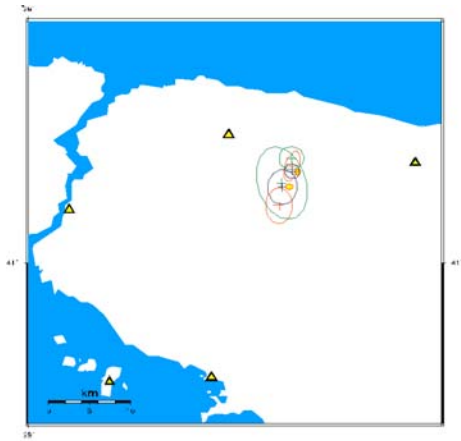
Vp,km/sec	Depth, km
<b>KOERI starting model 1</b>	
4.500	0.000
5.910	5.400
7.800	31.600
8.300	89.200
<b>KOERI modified model 2</b>	
3.800	0.000
5.700	2.100
6.100	4.000
6.800	25.000
7.800	31.600
8.300	89.200
<b>TUBITAK crustal model 3</b>	
2.25	0
5.70	1.0
6.10	6.0
6.80	20.0
8.05	33.0
8.07	40.0

We found a significant improvement in location and origin time estimation by applying the corrected crustal structure model 2 for the area (Table 3). The error estimation was made based on the ground-truth location and origin time of the blasts.

**Table 3. Location analysis of the Marmara blast No.4, 14.08.2002 (Hypo71 results).**

Type	Origin Time	OT error	Lat.	Lat. error	Long.	Long. error	Depth, km	Depth error	RMS	N of stations
GT data	10:24:17.7	-	41.116	-	29.295	-	0	-	-	-
Model 1	10:24:17.13	0.57	41.1541	0.038	29.2711	0.024	5.0	5.0	0.21	8
Model 2	10:24:18.02	0.32	41.1337	0.018	29.2827	0.012	0.2	0.2	0.1	8

An additional location calibration study, based on the Marmara GT0 blasts, was performed to estimate the accuracy of the seismic event locations and to reduce the size of error ellipses. The KOERI, TUBITAK, and ISTANBUL municipality stations, all within a distance of 100 km, were used. The existing KOERI velocity model was improved by examining the residuals of well-recorded events. A new velocity model 3 (Table 2) was obtained that reduced the error.



Three velocity models (Table 2) were used to calculate travel time residuals using the HYPOCENTER earthquake location software.

We compared the models using location errors and error ellipses (Figure 4). For event N1 the location obtained using model 1 (red) was shifted 3 km southwest with respect to the ground-truth location and is much larger than it is for models 2 and 3. The largest error ellipse was also obtained for model 1. The model 2 error ellipses are relatively small but biased and do not include the true location. Both small ellipses and unbiased locations are obtained with model 3 which should be used for earthquake location in this area.

**Figure 4. Horizontal error ellipses of the Marmara quarry blasts, obtained from the three models.**

### Israel Calibration Explosions

The closely spaced (~50 km) Dead Sea and 25-ton Rotem calibration explosions (Gitterman et al., 2002) were recorded at the same stations in Israel, Jordan, Cyprus, and Saudi Arabia (Figure 5) and provide observations for similar propagation paths; thus, allowing a comparison of source properties such as amplitudes, waveform, and spectral content of regional phases. In order to quantify the differences between these two calibration events, we examined the Power Spectral Density (PSD). For each component, 2 time windows were defined that corresponded to P- and S-waves. The windows begin at the P, S wave onsets and end 20 sec later.

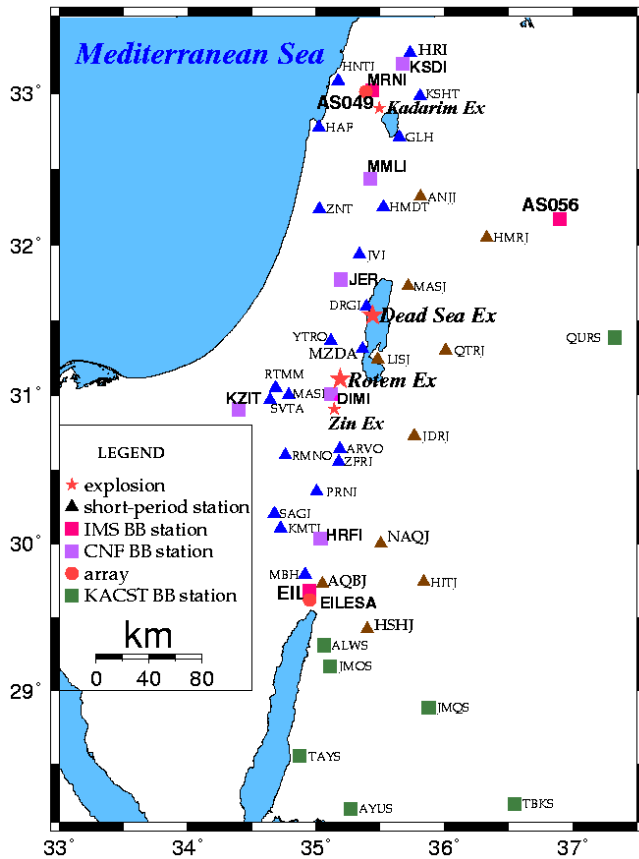


**Figure 5. Calibration explosions in Israel and observing stations.**

The spectra in Figure 6 exhibit higher power of P-waves (compared to S-waves) for both explosions. Spectral energy of both P and S waves for the land Rotem 25 ton blast is lower, compared to the underwater Dead Sea 0.5-ton shot, and shifted (by 1–1.5 Hz) to higher frequencies. However, the Rotem blast, which has a smaller local magnitude ( $M_L=3.0$ ) than the Dead Sea shot ( $M_L=3.1$ ), shows stronger P-wave amplitudes and better quality of the first arrival (though recorded at a larger distance).

The 25-ton Rotem blast records at several Saudi Arabia stations of the KACST network were recently obtained at the RELEMR workshop in Paris in October 2002. Clear signals were observed up to 346 km away (station TBKS, see Figure 7), but stations located at range >700 km did not show a signal. At three stations (QURS, ALWS, and TBKS) we have records of the Dead Sea 2-ton explosion,  $M_L=3.6$  (data for the 0.5-ton shot are not available). We also compared waveforms and spectral content of P and S-waves.

The P-wave spectra for ALWS station (Figure 8) shows lower energy for the Rotem blast than the 2-ton Dead Sea explosion in the range 1–6 Hz, and similar power at higher frequencies. It is noteworthy that spectral curves for the land blast show similar peaks and troughs to the underwater explosion, believed caused by the bubble pulse (Gitterman and Shapira, 2001). The reason for this is not clear.

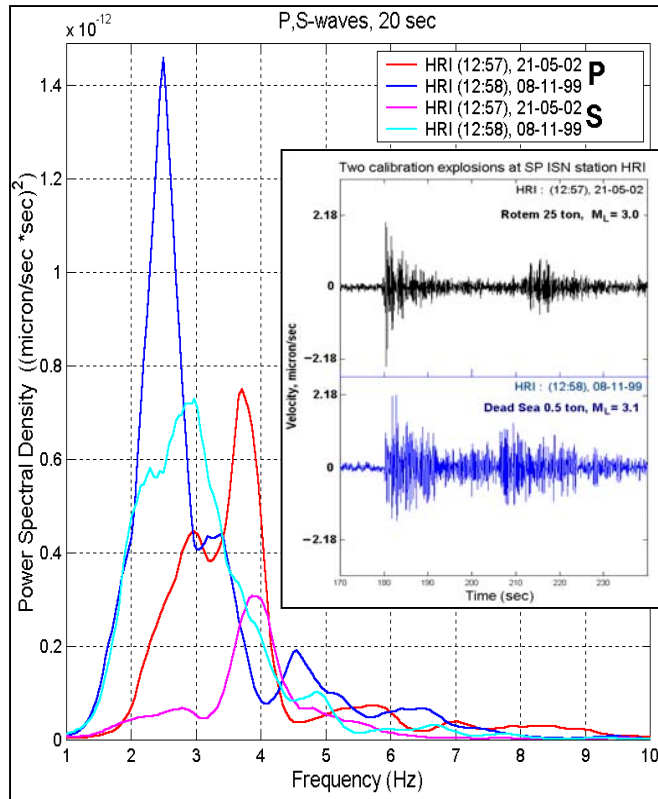


Figure 6. Seismograms and PSD of P and S waves at vertical short-period station HRI at distances 194 km from the Dead Sea 0.5 ton shot (08-11-99) and 245 km from the Rotem 25-ton shot (21-05-02).

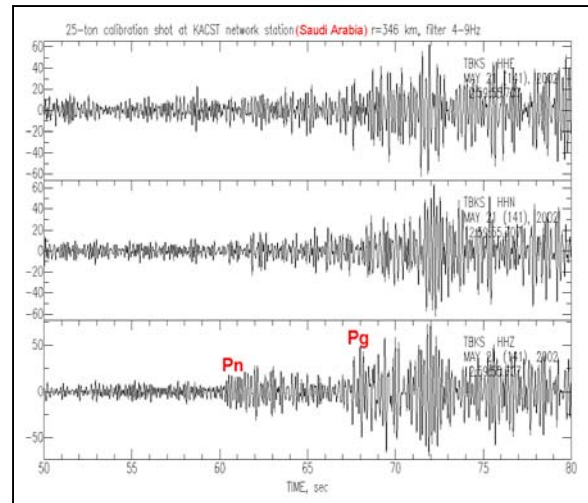


Figure 7. Clear regional phases P, Pg were found at BB station TBKS (Saudi Arabia) after narrow band-pass filtration (4-9 Hz).

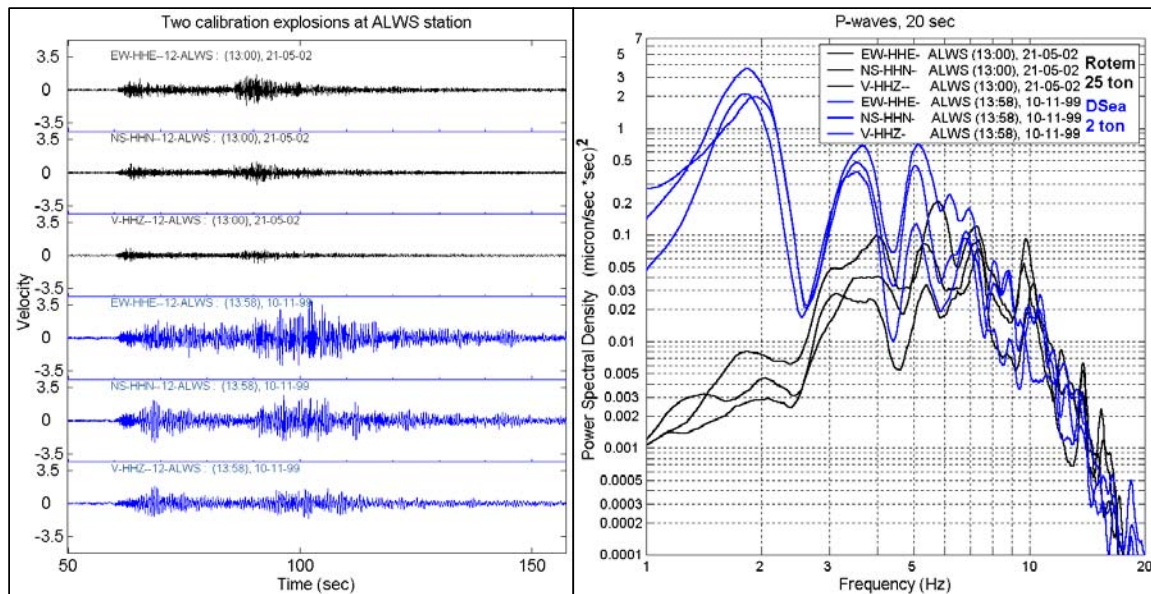


Figure 8. Seismograms and PSD of P waves at BB station ALWS (Saudi Arabia) at distances of 248 km from the 2-ton Dead Sea explosion (10-11-99) and 200 km from the 25-ton Rotem blast (21-05-02).

During the preparation of the second 25-ton calibration explosion in northern Israel, we conducted a number of controlled (GT0) test blasts at the Kadarim quarry (see Figure 5). The goals were: 1) ensuring the safety of nearby buildings in this densely populated area by measuring blast ground motions near the buildings and comparing them to predicted values from an empirical relationship and a code safety threshold; and 2) determining capability of the planned 25-ton explosion to provide the desired magnitude  $M_L=2.8-3.0$ . Data from these blasts will also be used to estimate attenuation, magnitude-yield relations, characterization of new seismic sources and local mining practices, and multi-station discrimination analysis.

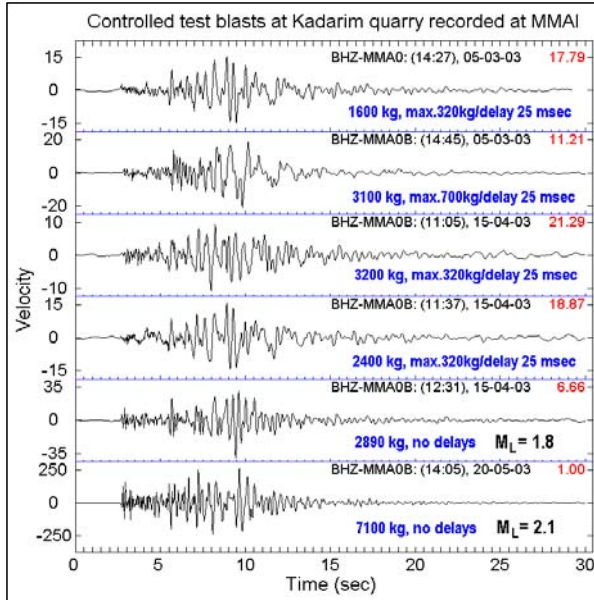


Figure 9. Records of controlled ripple-fired and instantaneous quarry blasts at central BB vertical element of the IMS array MMAI at Mt. Meron.

For the strongest blast the magnitude value was lower (2.1) than expected (2.4-2.5) for an instantaneous blast (Gitterman, 1998). Blast energy loss was caused by the small separation between the first hole and the bench face (2-3 m); this needs to be increased for the big calibration explosion.

We collected records of these blasts at the new IMS array MMAI (AS049) that started operation at Mt. Meron in early 2003 (Figure 9 {A: where is the Figure 8 callout?}). The blasts discussed above are located a short distance ( $r = 12.5$  km) from the array. We also conducted a controlled (routine) 11-ton blast (16.02.2003) in the Zin quarry, Negev (Figure 5), at  $r=237$  km. This first dataset of GT0 events at MMAI array can be used for regional calibration of this IMS station.

The Zin blast record at a close-in ( $\sim 1.3$  km) portable seismometer (see inset on Figure 10a) can be considered an approximation of the source spectrum, showing most of the energy in the range 2-6 Hz (Figure 10a). Background noise records at MMAI have most energy at lower frequencies (0.1-1 Hz). Band-pass filtration in the 2 – 10 Hz band provides significant improvement of the signal-to-noise ratio and reveals clear P and S waves for the 11-ton blast (see inset on Figure 10b).

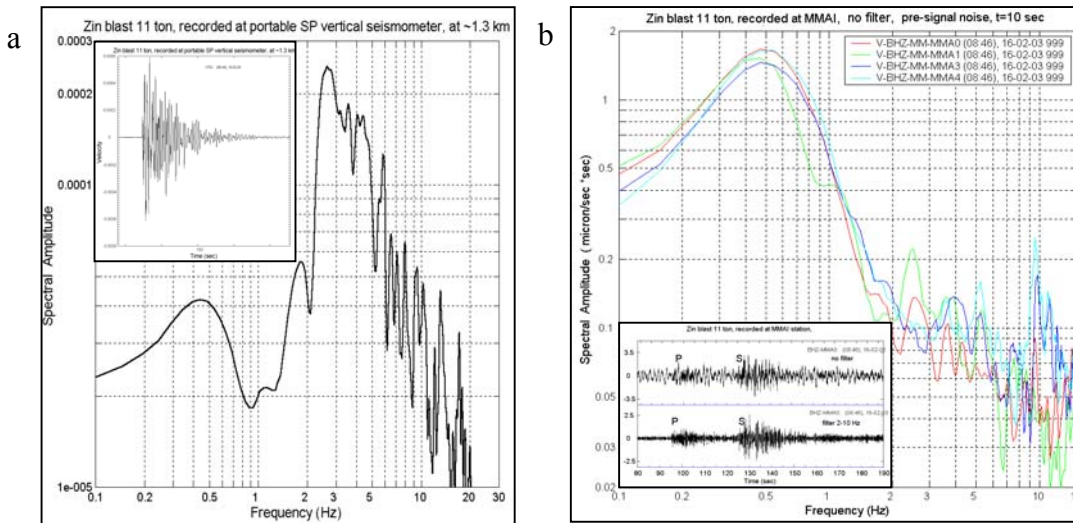


Figure 10. Spectral analysis of the near-source record of the Zin blast (a) and pre-signal noise (b) was used to improve SNR at MMAI records.

### Travel Time Evaluation

First arrival (P/Pn) travel time deviations relative to the IASPEI91 and local GII velocity models for the Rotem and Dead Sea calibration explosions were calculated and are presented in Figure 11. Travel time deviations for P waves relative the IASPEI91 and GII models are plotted on a map where color of the station symbol (triangle) corresponds to a delay value based on the palette.

The deviations show that at small distances (up to 90 km) the difference between observed and IASPEI91 travel time can be corrected by using the local (GII) velocity model. However, at the northern stations AS049 (212 km, IMS surrogate station), KSDI (235.3 km), and HRI (245 km) there is still a delay of ~1 sec. For the southern stations EIL and HRFI (120 km, 160 km) and the IMS station AS056 in Jordan, the respective negative delay was also observed. In general, for distances  $R > 125$  km, the difference between the two model travel times and the observations diminishes.

A difference ~1 sec is found in travel time corrections (relative to IASPEI91) for some Saudi Arabia stations (ALWS, TBKS, BDAS/TAYS) obtained from the closely spaced (~50 km) calibration shots: in the Rotem quarry (Figure 11 a) and in the Dead Sea (Figure 11 c). Note the Rotem quarry is in the Negev desert while the Dead Sea is in the Dead Sea fault zone, a different geological setting.

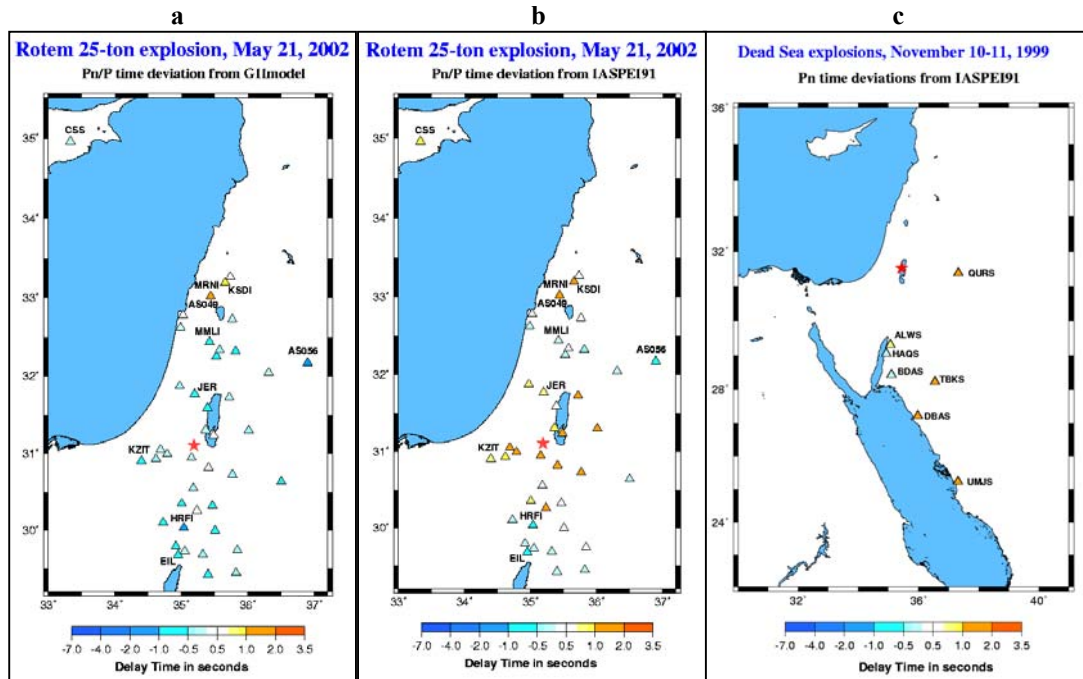


**Figure 11. Discrete regional map of Pn/Pg travel-time deviations for the Rotem (a, b) and Dead Sea (c) calibration explosions recorded at local network stations.**

### Computation of SSSCs for the Middle East-East Mediterranean Region

To improve the IMS event location in the region, we investigated Pn travel times calculated with the best existing 3-D velocity models compared to measured values from the GT events database. For this investigation we installed at GII the crust and mantle 3-D CUB1.0 velocity model, developed by the Geophysics Group of Colorado University (CU) Physics Department (Ritzwoller and Levshin, 1998), and the 2Dtracerdn software (Barmin et al., 2001). The CU 3-D model was obtained from inversion of broadband surface-wave dispersion data on a  $2^\circ \times 2^\circ$  grid and the application of a simple scaling relationship  $d(\ln V_p) = 0.5d(\ln V_s)$ . The rays and travel times (SSSCs) have been calculated up to 2,000 km distance for stations EIL, MRNI, and BRAR (see Figure 12).

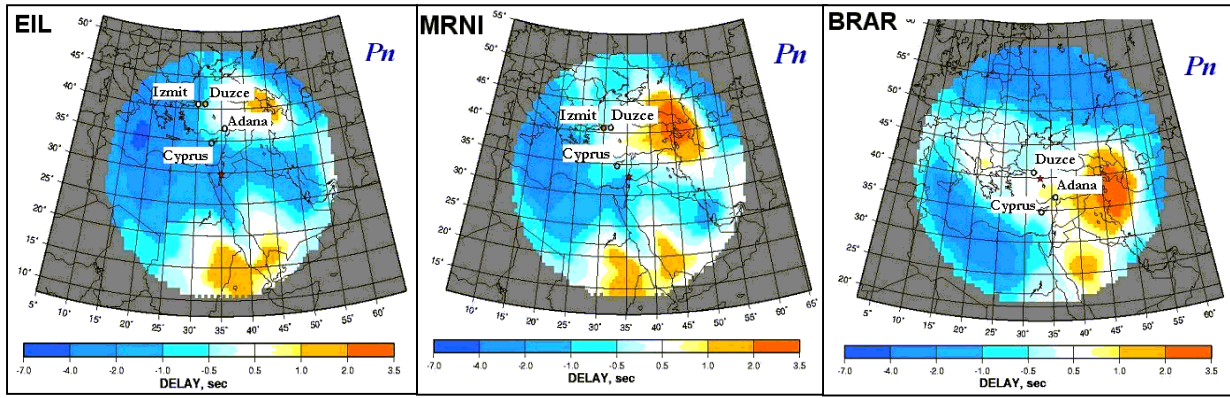


**Figure 12. SSSCs for Pn relative to IASPEI91, depth H=10 km, for the three IMS stations.**

The model-based travel time computations were compared to those obtained from arrival time measurements and hypocenter estimation of the GT events collected in the areas of Duzce, Izmit, Adana (Turkey), and Cyprus. The measured time delays for different GT events were calculated as:  $dM = TT - TT_{IASP91}$ , where  $TT = AT - OT$  - travel time, determined by the measured arrival time  $AT$  at the IMS stations EIL, MRNI, and BRAR with GT origin parameters  $OT$ ,  $Lat$ ,  $Long$ , and depth  $H$ , taken from the results of the relocation experiment (Pinsky et al, 2001). For calculation of the  $TT_{IASP91}$  we used the *ttimes* program (Kennett and Engdahl, 1991).

The  $dM$  values are averaged according to  $EdM = \sum k_j dM_i / \sum k_j$ , where weights  $k_j$  are determined by the SNR, and are depicted in Figure 12 as colored circles plotted on the contoured SSSCs from CUB 1.0, which are computed for the source depth  $H=10$  km.

Match of a circle and the background color indicates coincidence of the measured and CUB1.0 predicted travel times. For many cases we have good agreement between the measured and calculated SSSCs. However, there are a number of large discrepancies at various sites (see, for example, Duzce for EIL, Izmit for MRNI).

### **Pilot Performance Analysis for New IMS Array on Mt. Meron and a New Robust Beamformer**

The 16-element modern array AS049 (MMAI) has the potential to notably increase the nuclear test monitoring capability in the region (see Figure 13a). The array geometry (3.1-km long, 2.3-km wide) is shown in Figure 13b. Although this site is regarded as the best suited for this purpose in Israel and the array seismometers are deployed in deep boreholes for noise abatement, there is a significant level of noise generated by a number of technological sources in the area. Sporadic bursts are often seen on only one or several of the array channels, causing a non-stationary noise process. As a result of the mountainous character of the landscape, the geology around the array is very heterogeneous—leading to waveform distortions and random delays. Therefore, we immediately confronted a deficiency of signal coherency at mutually remote stations leading to both reduced detection capability and location accuracy.

To solve the problem we started to develop a new robust beamforming technique. In the frequency domain beamforming is equivalent to the calculation at each discrete frequency  $f$  a scalar product  $w = \mathbf{H}^* \mathbf{X}$ , where  $\mathbf{X}$  is a DFT vector of observations:  $\mathbf{X}^T = (x_1, x_2, \dots, x_M)$ , and  $\mathbf{H}$  is a vector of DFT plane wave delays:  $\mathbf{h}_m(k) = \exp(-i2\pi f \tau_m)$ , where plane wave time delay  $\tau_m = (dI_m, k)$ . For an ideal array without noise and signal distortion and an ideal plane wave coming with wave number vector  $k_0$ , vector  $\mathbf{X} = x_1 \mathbf{H}(k_0)$ , and, thus,  $w = M x_1$ .

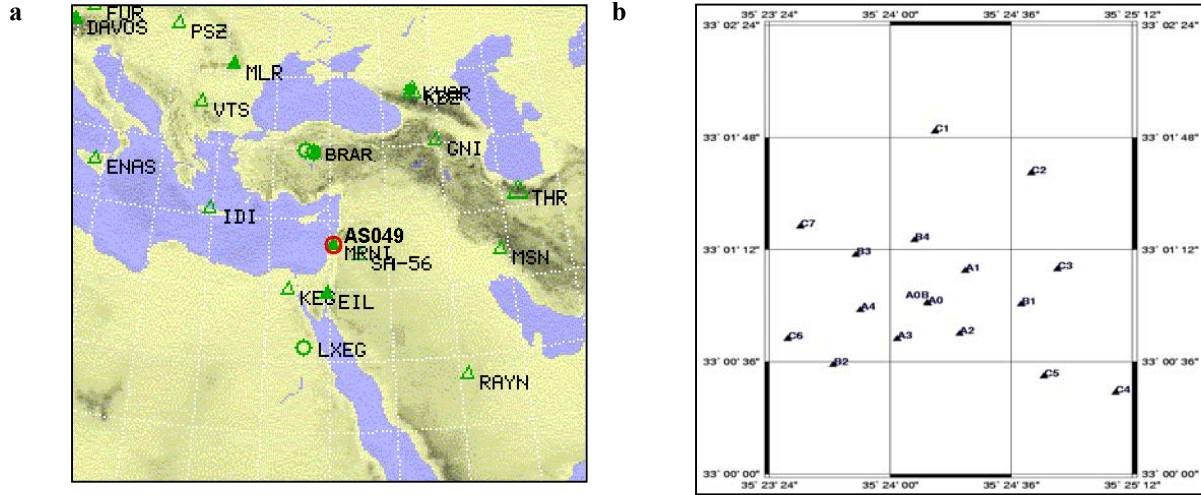


Figure 13. Location (a) and configuration (b) of the AS049 array, Mt. Meron, Israel

The wave number vector  $k_0$  is estimated by maximization of  $|w|^2$ . In fact, the assumption as stated above is rarely valid for all the array stations, thus reducing beamforming effectiveness, however, it may remain so for a subnetwork. Let us introduce a bell-shape function  $y=\varphi(t)$ :  $\{\varphi(0)=1, \varphi(t) \rightarrow 0 \text{ when } t \rightarrow \infty\}$  and compute the statistic:

$$v = \max_{\theta \in (0, 2\pi], k \in K, f \in \Phi} \sum_{m=1}^M \varphi[\arg(h_m^* x_m) - \theta], \quad (1)$$

where  $K$ - slowness range,  $\Phi$ - frequency range. In the ideal case  $v=M$ . In the adaptive beamforming case

$$W = H^* * F^{-1} X / (H^* F^{-1} H), \quad (2)$$

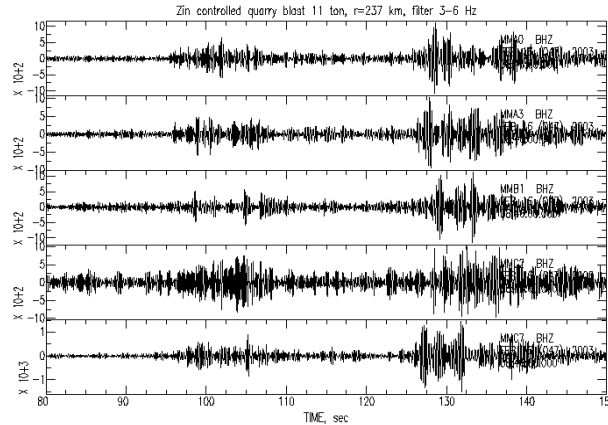


Figure 14. Five BP-filtered (3–6 Hz) channels of the \*AS049 array

where  $F$  is a noise spectral density matrix  $F = ENN^*$ . Since the denominator in (2) is a real number, then for computation statistic equivalent to (1) we should substitute  $x_m$  by components  $y_m$  of the vector  $Y = F^{-1}X$ , where  $F^{-1}$  is inverse or pseudo-inverse of matrix  $F$ . Thus, finally the target statistic is

$$u = \max_{\theta \in (0, 2\pi], k \in K, f \in \Phi} \sum_{m=1}^M \varphi[\arg(h_m^* y_m) - \theta] \quad (3)$$

We performed a pilot study of the robust beamforming based on observations of the controlled explosions at the Israel quarries mentioned above. An example of the analysis for the Zin quarry blast (ground truth azimuth  $186.5^\circ$ ) is presented in Figures 14 and 15.

Low SNR ( $\sim 1$ ) is observed at the array records, and first Pn arrivals can hardly be seen even after heavy BP filtering in the 3–6 Hz frequency band (see Figure 14). However, estimates of the azimuth  $Az$  and apparent velocity  $V$ , shown in the F-K diagram (Figure 15) at frequency  $F=1.9$  Hz, correspond well to the ground-truth values for both the conventional ( $Az=195^\circ$ ,  $V=6.4$  km/s) and “robust” beamforming (1) ( $Az=184.7$ ,  $V=8.3$  km/s) (see Figure 15 a, b). To demonstrate the stability of the “robust” beamforming, the channel B2 was distorted. The conventional beam failed, however, the “robust” beamforming result remained almost unchanged (see Figure 15 c, d).

### CONCLUSIONS AND RECOMMENDATIONS

Controlled quarry blasts are a relatively cheap and useful tool to deliver information needed for underground nuclear test monitoring, such as velocity models, travel time and azimuth corrections, characterization of the influence of propagation path and source on waveforms, and spectral contents, magnitudes, etc. Using data from controlled quarry blasts we improved the velocity model and event location in the Marmara region, Turkey, and provided calibration information for the IMS stations EIL and AS049 in Israel. The Kadarim quarry test blast series provided data for conducting a second large 25-ton calibration explosion in Northern Israel. Two calibration explosion sites, the Dead Sea shot point and the Rotem quarry, were close enough to assume different propagation paths for the close stations and similar propagation paths for the remote stations, allowing evaluation of source and path effects.

Spectral estimates of the signal from the Zin quarry explosion, Negev, at a close-in portable station and the AS049 array provided information to estimate the path effect of a 237-km segment along the Dead Sea fault. The explosion data were also used for apparent velocity and azimuth calibration and tuning of a new robust beamforming algorithm at the array. This pilot research revealed the high potential of the array to extract weak signals from noisy seismograms and showed the effectiveness of a robust approach in location of small events under difficult conditions of heterogeneity and impulsive cultural noise. The new technique showed promise; however, it is relatively time consuming and must contend with large stationary and mutually correlated noise. Further investigation will be devoted to calibrating azimuth and apparent velocity estimations around the array, development of the adaptive robust beamformer, and tuning of its parameters. A large statistical experiment is planned to estimate the effectiveness of the new technique under various conditions.

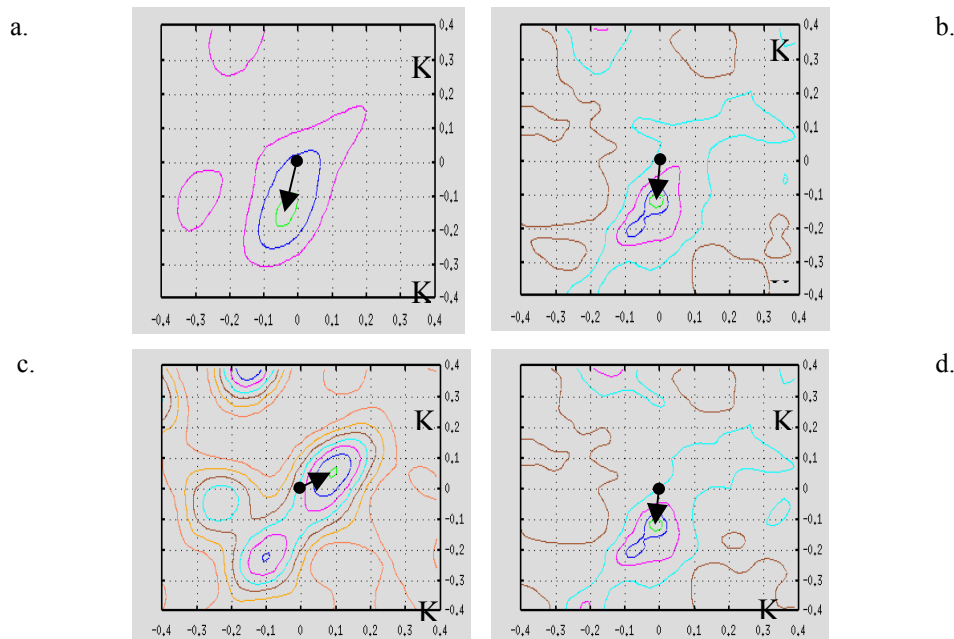


**Figure 15. Comparison of conventional (a, c) and robust (b, d) beamforming in the F-K domain, applied to the Zin explosion ( $Az=186.5$ ,  $V=7.9$  km/s) at a time point  $t=92$  sec, time window length  $l=3.2$  sec, frequency 1.9 Hz, before (a, b) and after (c, d) the distortion of the B2 channel signal.**

**REFERENCES**

- Barmin, M.P., M.H. Ritzwoller, and A.L. Levshin (2001), A fast and reliable method for surface wave tomography, *Pure and Appl. Geophys.*, Volume 158, Issue 8, 1351-1375.
- Gitterman, Y., V. Pinsky, A. Shapira, M. Ergin, D. Kalafat, G. Gurbuz, K. Solomi (2002), "Improvement in detection, location and identification of small events through joint data analysis by seismic stations in the Middle East/Eastern Mediterranean region," *Proceedings of the 24th Seismic Research Review – Nuclear Explosion Monitoring: Innovation and Integration*, 17-19 September 2002, Ponte Vedra Beach, Florida, pp. 271-282.
- Gitterman, Y. and A. Shapira (2001), Dead Sea Seismic Calibration Experiment contributes to CTBT Monitoring, *Seismological Research Letters*, Vol. 72, Num. 2, March/April 2001, 159-170.
- Gitterman, Y. (1998), Magnitude yield correlation and amplitude attenuation of chemical explosions in the Middle East, *Proceedings of the 20<sup>th</sup> Annual Seismic Research Symposium on Monitoring a Comprehensive Nuclear Test Ban Treaty*, Santa Fe, Sept.21-23, 1998, 302-311.
- Kennett, B.L.N. and E.R. Engdahl (1991), Travel times for global earthquake location and phase identification, *Geophys. J. Int.*, 105, 469 - 465.
- Pinsky, V., Gitterman, Y., Goldshmidt, V., Shapira, A. (2001). Collection of regional calibration data within the area around the Israel Seismic Network. CTBTO Calibration Program - Phase I. Annual Report on Contract 00/20/5024. November 2001, GIRep. 571/155/01(2), 105 p.
- Ritzwoller, M.H., and A.L. Levshin (1998). Eurasian surface wave tomography: Group velocities, *J. Geophys. Res.*, 103, 4839 - 4878.